Gayaz Khakimzyanov
Institute of Computational Technologies, Novosibirsk, Russia

Denys Dutykh
CNRS, Université Savoie Mont Blanc, France

arXiv:1511.02770v2 [math.NA] 28 Apr 2016

On supraconvergence phenomenon for second order centered finite differences on non-uniform grids

arXiv.org / HAL

Last modified: April 29, 2016

On supraconvergence phenomenon for second order centered finite differences on non-uniform grids

Gayaz Khakimzyanov and Denys Dutykh*

Abstract. In the present note we consider an example of a boundary value problem for a simple second order ordinary differential equation, which may exhibit a boundary layer phenomenon depending on the value of a free parameter. To this equation we apply an adaptive numerical method on redistributed grids. We show that usual central finite differences, which are second order accurate on a uniform grid, can be substantially upgraded to the fourth order by a suitable choice of the underlying non-uniform grid. Moreover, we show also that some other choices of the nodes distributions lead to substantial degradation of the accuracy. This example is quite pedagogical and we use it only for illustrative purposes. It may serve as a guidance for more complex problems.

Key words and phrases: finite differences; non-uniform grids; boundary layer; boundary value problems; supraconvergence

MSC: [2010]65N06 (primary), 76M20, 65L10 (secondary)

* Corresponding author.

Contents

1 Introduction **4**

2 The boundary value problem **5**

2.1 Discretization on a uniform grid 6

2.2 Non-uniform adaptive grids 7

2.3 Adaptive mesh generation 8

Example 10

Generalizations 10

3 Numerical results **11**

4 Explanations **14**

5 Discussion **15**

Acknowledgments 16

References **16**

1. Introduction

The boundary layer phenomena are present in many applications, in particular in Fluid Mechanics and Aerodynamics [22]. For instance, the very successful design of AIRBUS A320's wing is mainly due to the potential flow theory with appropriate boundary layer corrections [19]. Nowadays this problem is addressed mainly with numerical techniques and it represents serious challenges.

Some numerical approaches to address the boundary layer problem have been proposed since the early 60's. Historically, probably homogeneous schemes on uniform [25] and non-uniform [26] meshes were proposed first by TIKHONOV and SAMARSKII. Later, IL'IN proposed the so-called exponential-fitted schemes [14, 20], which were generalized recently to finite volumes as well (see *e.g.* [9]). The idea of IL'IN consisted in introducing the so-called *fitting factor* into the scheme and requiring that a particular exact solution satisfies the difference equation exactly. We can also mention two pioneering references where the moving grids were first applied to unsteady problems in shallow water flows [24] and in gas dynamics [1]. The uniform convergence of monotone finite difference operators for singularly perturbed semi-linear equations was shown in [10]. We refer to [15] for a general review of numerical methods in the boundary layer theory.

In [19, pp. 585–586] one can read:

> *I am convinced that it should be possible to develop a general theory of the relation between the grid, the governing equations and the specific solution being computed, but only very hazy ideas how to bring such a theory about.*

Our study is a little attempt towards this research direction. Namely, in the present manuscript we consider a singularly perturbed linear second order elliptic ODE as a model equation which exhibits the boundary layer phenomenon. In accordance with I. M. GELFAND principle, we took the simplest non-trivial example to illustrate our point. The goal is to propose a numerical method for such problems, which is able to solve approximatively this problem with an accuracy independent of the value of the perturbation parameter [20]. In the beginning we explain why the classical central finite differences on a *uniform mesh* is not working in practice, even if this method is fully justified from the theoretical point of view with well-known stability and convergence properties [21]. Then, we propose a non-uniform equidistributed grid and we show that the same central difference scheme converges with the fourth order rate on this family of successively refined grids. So, just by changing the distribution of nodes in a smart way one can gain two extra orders of the accuracy! The logarithmically-distributed grids were proposed by BAKHVALOV [2]. However, they were shown to converge inevitably with the same second order rate (see [21] for the proof).

Non-uniform grids can be used also to compute numerically blow-up solutions as in the nonlinear Schrödinger equation [4]. See also [6] for a general review of these techniques. There is a related idea of constructing non-uniform grids in order to preserve some or all symmetries of the continuous equation at the discrete level as well [7]. We can only deplore that the authors of [7] did not study theoretically the stability and convergence

of the scheme depending on symmetry preservation abilities. The same idea holds for invariants [4, 8] and asymptotics [5, 27]. In the present study we focus essentially on the scheme approximation order depending on the underlying (non-uniform) grid.

The phenomenon of supraconvergence phenomenon of central finite difference schemes is well known and it was studied rigorously in one spatial dimension in [3] and the 2D case was considered in [12]. However, to our knowledge the increase from the second to the fourth order has never been reported in the literature. The *super-supraconvergence* reported in this manuscript is the first example in this novel direction. As Strang & Iserles [23] discovered the link between the stability and the stencil of a numerical scheme, here we establish a link between the scheme's convergence order and the underlying grid. In particular, we show that some thouroughly chosen nodes distributions lead to the substantial improvement of the numerical solution accuracy (for a fixed scheme). We show also that some other grid choices (appearing admissible from the first sight) may totally degrade the solution accuracy. These illustrations should serve as an indication for more complex problems.

The present manuscript is organized as follows. The BVP under consideration is described in Section 2. The classical discretization is described in Section 2.1, while the scheme on a general non-uniform grid is provided in Section 2.2. A practical equidistribution method to construct the grids is explained in Section 2.3. A series of numerical experiments on various non-uniform grids is presented in Section 3 and some theoretical insight into these results is given in Section 4. Finally, the article is completed by outlining the main conclusions and perspectives of the present study in Section 5.

2. The boundary value problem

Consider the following linear Boundary Value Problem (BVP) for an ordinary differential equation $\mathscr{L}u = 0$ of the second degree with Dirichlet-type boundary conditions on the segment $\mathcal{I} = [0, \ell]$:

$$\mathscr{L}u := -\frac{\mathrm{d}^2 u}{\mathrm{d}x^2} + \lambda^2 u = 0, \qquad u(0) = \mathrm{e}^{-\lambda\ell}, \quad u(\ell) = 1, \tag{2.1}$$

where λ is a model parameter. It can be readily checked that the following function of x solves exactly the BVP (2.1):

$$u(x) = \mathrm{e}^{\lambda(x\,-\,\ell)}. \tag{2.2}$$

However, we shall proceed as if the analytical solution (2.2) were not known. It will serve us only to assess the quality of a numerical solution. The peculiarity here is that for sufficiently large values of parameter $\lambda \gg 1$ the solution (2.2) shows a boundary layer type behaviour in the vicinity of the point $x = \ell$. It is illustrated in Figure 1. Similar phenomena occur in Fluid Mechanics where they are of capital importance *e.g.* in Aerodynamics [22]. It justifies the choice of the problem (2.1) in our study.

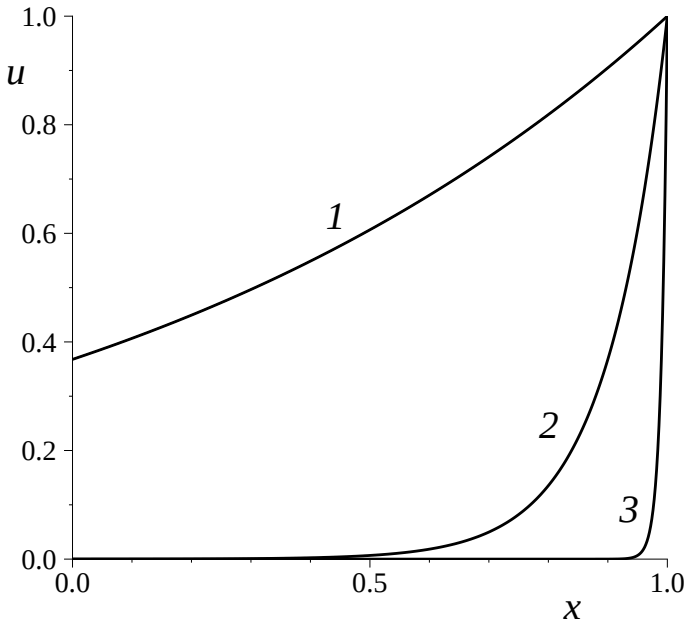

Figure 1. *Exact solutions* (2.2) *for* $\ell = 1$ *and various values of parameter* λ*: (1)* — $\lambda = 1$*, (2)* — $\lambda = 10$*, (3)* — $\lambda = 100$*.*

Usually the problem (2.1) is rewritten in the literature by introducing a small parameter $\varepsilon := 1/\lambda^2$:

$$-\varepsilon \frac{\mathrm{d}^2 u}{\mathrm{d}x^2} + u = 0.$$

Thus, we have a singularly-perturbed Sturm-Liouville problem [18].

2.1. Discretization on a uniform grid

Consider a uniform discretization of the segment $\mathcal{I}$ in N equal segments $\mathcal{I}_h$ with boundaries located at $\{x_j = j\Delta x\}_{j=0}^{N}$, $\Delta x = \frac{\ell}{N}$. The finite difference analogue $\mathscr{L}^h u_h = 0$ of differential equation (2.1) is

$$\mathscr{L}_j^h\{u_j\} = -\frac{u_{j+1} - 2u_j + u_{j-1}}{\Delta x^2} + \lambda^2 u_j = 0, \qquad j = 1, \ldots, N-1, \tag{2.3}$$

together with Dirichlet-type boundary conditions:

$$u_0 = \mathrm{e}^{-\lambda \ell}, \qquad u_N = 1.$$

It is well known that this scheme has the second order accuracy, as it follows from the local consistency error analysis:

$$e_j^h := \mathscr{L}_j^h\{u(x_j)\} = u_{xxxx}(x_j)\frac{\Delta x^2}{12} + \mathcal{O}(\Delta x^4) = \lambda^4 \mathrm{e}^{\lambda(x_j - \ell)}\frac{\Delta x^2}{12} + \mathcal{O}(\Delta x^4).$$

From the last formula we can already draw some preliminary conclusions:

- The proportionality constant grows as the fourth power of the parameter λ, which can take potentially large values in practically important situations.
- The ratio between the consistency error in the vicinity of $x = \ell$ and $x = 0$ is $\approx \exp(\lambda\ell)$.

We would like to mention that the stability proof of scheme (2.3) can be found *e.g.* in [13]. So, according to Lax–Richtmyer equivalence theorem [17], the scheme (2.3) is convergent as $\Delta x \to 0$ and the convergence rate is equal to the approximation order (*i.e.* two in this particular case). However, despite all these good properties the scheme (2.3) is not usable in practice because of two practical drawbacks mentioned above (they are all related to the asymptotic limit $\lambda \to \infty$ and the boundary layer phenomenon). Please, note however that the convergence is established for a fixed value of the parameter λ.

2.2. Non-uniform adaptive grids

In order to cope with the shortcomings mentioned above, we turn to non-uniform grids by preserving the simplicity of the second-order central discretization (2.3). Let $Q = [0, 1]$ be the reference domain and consider a bijective mapping from Q to $\mathcal{I}$:

$$x(q) : \; q \in Q \; \mapsto \; \mathcal{I}. \tag{2.4}$$

We require that the boundary points map into each other:

$$x(0) \; = \; 0, \qquad x(1) \; = \; \ell.$$

We shall also assume that the Jacobian $J(q)$ of mapping (2.4) is bounded from below and above by some positive constants:

$$0 \; < \; J_m \; \leqslant \; J(q) \; := \; \frac{\mathrm{d}x(q)}{\mathrm{d}q} \; \leqslant \; J_M \; < \; \infty, \qquad \forall q \in Q. \tag{2.5}$$

The reference domain can be discretized into N equal elements Q_h by nodes $\{q_j = jh\}_{j=0}^{N}$, $h = 1/N$. Strictly speaking, for our numerical purposes we can be satisfied with the knowledge of the discrete mapping $x^h : Q_h \mapsto \mathcal{I}_h$. From condition (2.5) (more precisely from this part: $0 < J_m \leqslant J(q)$) follows that the steps of the non-uniform mesh $\mathcal{I}_h$ are necessarily positive *i.e.*

$$h_{j+1/2} \; := \; x_{j+1} \; - \; x_j \; > \; 0, \qquad j \; = \; 0, \ldots, N-1. \tag{2.6}$$

From the condition $J(q) \leqslant J_M < \infty$ follows that

$$h_{\max} \; := \; \max_{j=0,\ldots,N-1} h_{j+1/2} \; \leqslant \; J_M h \; \to \; 0, \qquad h \; \to \; 0.$$

We note also that if the Jacobian $J(q) \equiv \text{const}$ (or equivalently the mapping $x(q)$ is linear), the resulting mesh $\mathcal{I}_h$ is uniform. This case is not very interesting from the adaptivity point of view. Any other map $x(q)$, which satisfies the boundary conditions with (2.5) defines a valid non-uniform grid $\mathcal{I}_h$. However, not all of them are equally interesting from

the numerical point of view. Some practical methods to compute solution-adapted meshes will be discussed below in Section 2.3.

Equation (2.1) can be posed on the reference domain Q:

$$-\frac{1}{J}\frac{\mathrm{d}}{\mathrm{d}q}\left(\frac{1}{J}\frac{\mathrm{d}v}{\mathrm{d}q}\right) + \lambda^2 v = 0, \tag{2.7}$$

with the same boundary conditions $v(0) = \mathrm{e}^{-\lambda\ell}$, $v(1) = 1$. Here v is the composed function $v(q) := u \circ x = u\big(x(q)\big)$. Now equation (2.7) is posed on domain Q and, thus, it can be discretized on the *uniform* grid Q_h as follows

$$-\frac{1}{hJ_j}\left[\frac{v_{j+1} - v_j}{hJ_{j+1/2}} - \frac{v_j - v_{j-1}}{hJ_{j-1/2}}\right] + \lambda^2 v_j = 0, \qquad j = 1, \ldots, N-1, \tag{2.8}$$

where the Jacobian J is computed as

$$J_{j+1/2} := \frac{x_{j+1} - x_j}{h}, \quad J_{j-1/2} := \frac{x_j - x_{j-1}}{h}, \quad J_j := \frac{J_{j-1/2} + J_{j+1/2}}{2}.$$

Difference equations (2.8) have to be completed with corresponding boundary conditions

$$v_0 = \mathrm{e}^{-\lambda\ell}, \qquad v_N = 1.$$

The last scheme (2.8) can be equivalently rewritten on the non-uniform grid $\mathcal{I}_h$:

$$-\frac{1}{h_j}\left[\frac{u_{j+1} - u_j}{h_{j+1/2}} - \frac{u_j - u_{j-1}}{h_{j-1/2}}\right] + \lambda^2 u_j = 0, \qquad j = 1, \ldots, N-1, \tag{2.9}$$

where $h_{j\pm1/2}$ were defined in (2.6) and

$$h_j := \frac{h_{j-1/2} + h_{j+1/2}}{2}.$$

2.3. Adaptive mesh generation

The finite difference scheme on the transformed uniform Q_h and non-uniform $\mathcal{I}_h$ grids were formulated in the previous Section. We choose the equidistribution method presented below. A similar nodes redistribution method was explained in details for time-dependent hyperbolic problems in a companion paper [16]. The exposition below is simpler since we deal with a stationary problem. Thus, we do not have here an additional complication of nodes motion in space and in time, which was addressed in [16].

A non-uniform grid $\mathcal{I}_h$ is given if we construct somehow the mapping $x(q) : Q \mapsto \mathcal{I}$ and evaluate it in the nodes of the uniform grid, *i.e.* $\mathcal{I}_h = x(Q_h)$. In the equidistribution method it is proposed that the desired mapping $x(q)$ is obtained as a solution to the following nonlinear elliptic problem

$$\frac{\mathrm{d}}{\mathrm{d}q}\left[\omega(x)\frac{\mathrm{d}x}{\mathrm{d}q}\right] = 0, \qquad x(0) = 0, \quad x(1) = \ell, \tag{2.10}$$

where $\omega(x)$ is the so-called *monitor* function. In order to have a well-posed problem (2.10), the function $\omega(x)$ has to be sufficiently smooth and positive valued. The equidistribution principle can be readily obtained by integrating (2.10) once in q-space

$$\omega\big(x(q)\big)\, J(q) \;\equiv\; C \;=\; \text{const}, \qquad \forall q \in Q, \tag{2.11}$$

and another time in x-space on the element $[x_j, x_{j+1}]$:

$$\int_{x_j}^{x_{j+1}} \omega(x)\,\mathrm{d}x \;=\; Ch \;=\; \text{const}. \tag{2.12}$$

The last identity explains the name of the equidistribution principle, *i.e.* the quantity $\omega(x)$ is distributed uniformly over the cells $\mathcal{I}_h$. In other words, in the areas where $\omega(x)$ takes high values, the elements $[x_j, x_{j+1}]$ are smaller in order to satisfy the condition (2.12). The constant C is not arbitrary and it can be computed exactly:

$$C \;=\; \int_0^1 \omega\big(x(q)\big)\, J(q)\,\mathrm{d}q \;=\; \int_0^\ell \omega(x)\,\mathrm{d}x.$$

In practice, one has to choose the monitor function $\omega(x)$ and solve the nonlinear elliptic Boundary Value Problem (BVP) (2.10) in order to obtain the required mapping $x(q)$. Since we need to know only this mapping in the grid nodes q_j, the problem (2.10) can be discretized using the central finite differences as well

$$\frac{1}{h}\left[\omega(x_{j+1/2})\,\frac{x_{j+1} - x_j}{h} - \omega(x_{j-1/2})\,\frac{x_j - x_{j-1}}{h}\right] \;=\; 0, \qquad j \;=\; 1,\dots,N-1, \tag{2.13}$$

with discrete boundary conditions $x_0 = 0$, $x_N = \ell$. Equations (2.13) are solved iteratively using the following linearization:

$$\frac{1}{h}\left[\omega(x_{j+1/2}^{(n)})\,\frac{x_{j+1}^{(n+1)} - x_j^{(n+1)}}{h} - \omega(x_{j-1/2}^{(n)})\,\frac{x_j^{(n+1)} - x_{j-1}^{(n+1)}}{h}\right] \;=\; 0, \qquad n \in \mathbb{N}.$$

The iterations are continued until the convergence within a prescribed tolerance is achieved. The linearized equations can be solved efficiently using the tridiagonal matrix algorithm [11].

A solution $\{x_j\}_{j=0}^N$ to the nonlinear BVP (2.13) satisfies the discrete version of the equidistribution principle (2.12):

$$\omega(x_{j+1/2})\,\frac{h_{j+1/2}}{h} \;=\; C_h \;=\; \text{const}, \qquad j \;=\; 0,1,\dots,N-1,$$

or equivalently

$$\omega(x_{j+1/2})\, J_{j+1/2} \;=\; C_h \;=\; \text{const}, \qquad j \;=\; 0,1,\dots,N-1.$$

The last identity is called the *discrete equidistribution principle*.

2.3.1 Example

In order to illustrate the use of the equidistribution principle in practice, we make the following choice of the monitor function

$$\omega(x) = \big(u_{xxx}\big)^{\frac{1}{4}} \propto \big(u_x\big)^{\frac{1}{4}}, \qquad x \in \mathcal{I}, \tag{2.14}$$

where $u(x)$ is the boundary layer solution (2.2). The proportionality $u_{xxx} \propto u_x$ follows from equation (2.1). In this case the nonlinear BVP (2.10) can be solved exactly by using the equidistribution principle (2.11), with constant

$$C = \int_0^{\ell} \lambda^{\frac{3}{4}} \mathrm{e}^{\frac{\lambda(x-\ell)}{4}} \,\mathrm{d}x = \frac{4}{\lambda^{\frac{1}{4}}}\big(1 - \mathrm{e}^{-\frac{\lambda\ell}{4}}\big).$$

Consequently, (2.11) reads

$$\lambda^{\frac{3}{4}} \mathrm{e}^{\frac{\lambda(x-\ell)}{4}} \frac{\mathrm{d}x}{\mathrm{d}q} = \frac{4}{\lambda^{\frac{1}{4}}}\big(1 - \mathrm{e}^{-\frac{\lambda\ell}{4}}\big).$$

From the last equation the mapping $x(q)$ can be found exactly

$$x(q) = \ell + \frac{4}{\lambda} \ln\big(q + (1-q)\,\mathrm{e}^{-\frac{\lambda\ell}{4}}\big).$$

Below it will become clear why we pay a special attention to this particular distribution of the nodes.

2.3.2 Generalizations

Example shown above can be easily generalized by taking the following monitor function:

$$\omega_\beta(x) = \big(u_x(x)\big)^{\beta}, \qquad \beta \in \mathbb{R}_0^+, \qquad x \in \mathcal{I}. \tag{2.15}$$

By performing the same computations as in the example above, one can show that this monitor function $\omega_\beta(x)$ yields the following mapping between the reference domain Q and computational domain $\mathcal{I}$:

$$x(q) = \begin{cases} \ell + \frac{1}{\beta\lambda} \ln\big[q + (1-q)\,\mathrm{e}^{-\beta\lambda\ell}\big], & \beta \neq 0, \\ q\ell, & \beta = 0. \end{cases} \tag{2.16}$$

For instance, one can see that the case $\beta = 0$ yields a uniform distribution of the nodes, which is not very interesting in view of generating adaptive redistributed meshes. Below we shall consider also a particular case when $\beta = \frac{1}{2}$, which gives the mapping $x(q)$ given by

$$x(q) = \ell + \frac{2}{\lambda} \ln\big[q + (1-q)\,\mathrm{e}^{-\frac{\lambda\ell}{2}}\big].$$

N	$\omega = 1$		$\omega = \big(u_x(x)\big)^{1/4}$		$\omega = \big(u_x(x)\big)^{1/2}$		$\omega = \big(u_x(x)\big)^{2}$	
	$\|\varepsilon_h\|_\infty$	p	$\|\varepsilon_h\|_\infty$	p	$\|\varepsilon_h\|_\infty$	p	$\|\varepsilon_h\|_\infty$	p
10	$0.141 \cdot 10^{-1}$	—	$0.146 \cdot 10^{-4}$	—	$0.456 \cdot 10^{-2}$	—	0.193	—
20	$0.375 \cdot 10^{-2}$	1.93	$0.883 \cdot 10^{-6}$	4.04	$0.101 \cdot 10^{-2}$	2.17	0.137	0.49
40	$0.953 \cdot 10^{-3}$	1.96	$0.548 \cdot 10^{-7}$	4.01	$0.220 \cdot 10^{-3}$	2.20	$0.960 \cdot 10^{-1}$	0.49
80	$0.239 \cdot 10^{-3}$	2.0	$0.342 \cdot 10^{-8}$	4.0	$0.512 \cdot 10^{-4}$	2.10	$0.668 \cdot 10^{-1}$	0.49
160	$0.599 \cdot 10^{-4}$	2.0	$0.214 \cdot 10^{-9}$	4.0	$0.127 \cdot 10^{-4}$	2.0	$0.463 \cdot 10^{-1}$	0.49
320	$0.150 \cdot 10^{-4}$	2.0	$0.136 \cdot 10^{-10}$	3.97	$0.317 \cdot 10^{-5}$	2.0	$0.319 \cdot 10^{-1}$	0.59
640	$0.374 \cdot 10^{-5}$	2.0	$0.836 \cdot 10^{-12}$	4.03	$0.792 \cdot 10^{-6}$	2.0	$0.220 \cdot 10^{-1}$	0.59

Table 1. *Numerical estimation of the convergence order of the scheme (2.8) for different choices of the monitor function $\omega(x)$. The computations are performed for $\ell = 1$ and $\lambda = 10$.*

3. Numerical results

In order to measure the quality of the numerical solution we compute its 'distance' to the reference solution given by (2.2):

$$\|\varepsilon_h\|_\infty \equiv \|u_h - (u)_h\|_\infty = \max_{0 \leqslant j \leqslant N} |u_j - u(x_j)|.$$

The convergence order p of a scheme can be estimated numerically as

$$p = \log_2 \left[\frac{\|\varepsilon_h\|_\infty}{\|\varepsilon_{h/2}\|_\infty} \right].$$

The parameter p has to be computed on a sequence of refined meshes to have a more robust estimation.

The numerical results are presented in Table 1 for various choices of the monitor function of the general form (2.15). The corresponding non-uniform meshes $\{x_j = x(q_j)\}_{j=0}^N$ were computed analytically above in (2.16). The choice of the monitor function $\omega(x) \equiv 1$ (*i.e.* $\beta = 0$) corresponds to a uniform grid and in this case we recover the theoretical 2^{nd} order convergence. However, the main focus of this study is on non-uniform grids. The most surprising result is the performance of the monitor function $\omega(x) = \big(u_x(x)\big)^{1/4}$. In this case we observe a fair 4^{th} order convergence! When the monitor function is changed to $\omega(x) = \big(u_x(x)\big)^{1/2}$ we come back to the 2^{nd} order convergence, even if the error norm $\|\varepsilon_h\|_\infty$ is approximatively 10 times lower. However, the most catastrophic results are observed for $\omega(x) = \big(u_x(x)\big)^{2}$, since the convergence order falls down to $p = \frac{1}{2}$. This distribution of nodes is certainly to be avoided in practical numerical simulations.

It is important to see how the error is distributed along the computational domain $\mathcal{I}$. For the same choices of the monitor function $\omega_\beta(x)$ it is depicted in Figure 2. One can see that the uniform grid leads to exponentially inaccurate results in the boundary layer

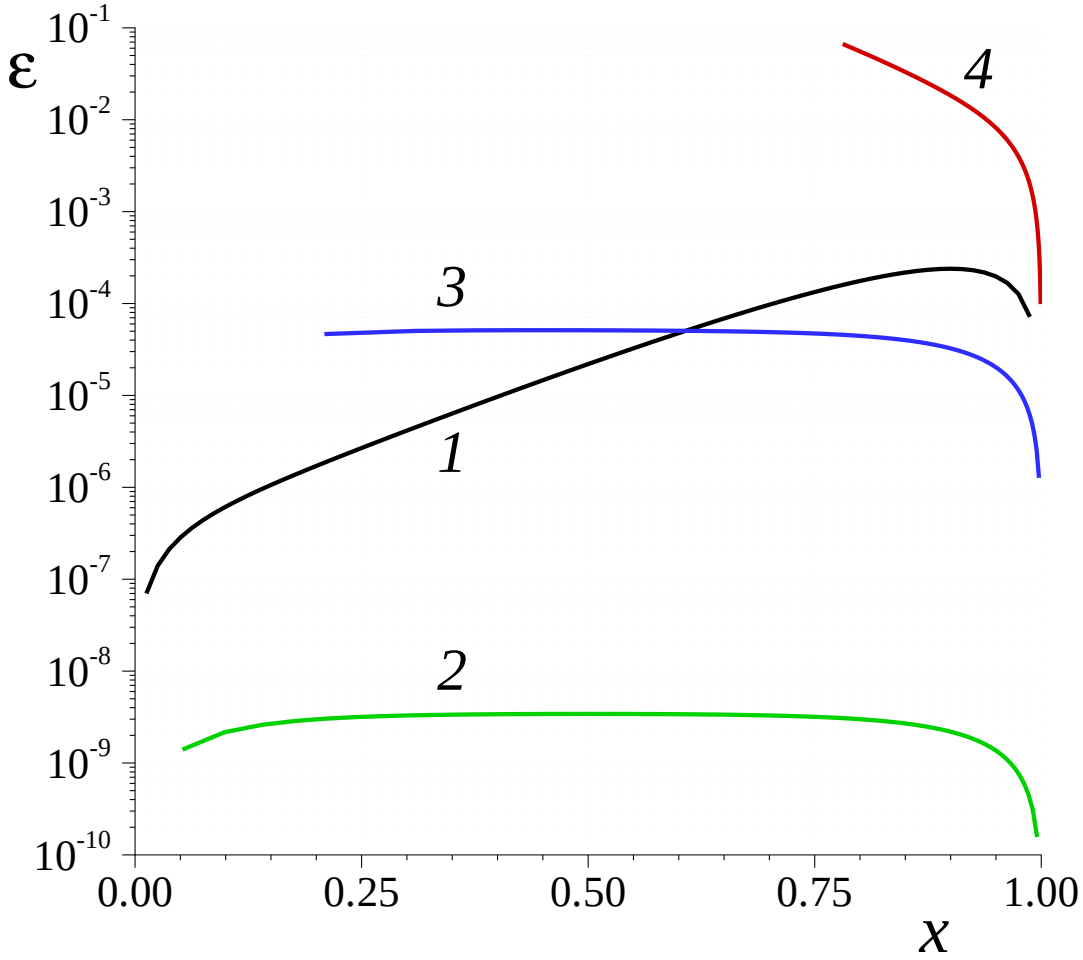

Figure 2. *Distribution of the numerical error in the computational domain for various choices of the monitor function $\omega(x)$: (1) — $\omega(x) \equiv 1$ (*i.e.* the uniform grid, (2) — $\omega(x) = \big(u_x(x)\big)^{\frac{1}{4}}$ (optimal case), (3) — $\omega(x) = \big(u_x(x)\big)^{\frac{1}{2}}$, (4) — $\omega(x) = \big(u_x(x)\big)^{2}$. The problem parameters are $\ell = 1$, $\lambda = 10$ and only $N = 80$ nodes are used.*

(*i.e.* the vicinity of $x = \ell$), despite its good theoretical properties on the paper. Without any surprise the supraconvergent case of $\omega_{1/4}(x)$ leads the lowest absolute error. However, it is surprising to see that $\omega_{1/2}(x)$ suppresses the main drawback of the uniform mesh (while preserving its order of convergence) — the error does not explode anymore in the boundary layer. Finally, one can see that $\omega_2(x)$ is a poor choice since it leads to huge errors on the left end of the computational domain (*i.e.* $x = 0$). What happens is that we put too many nodes in the boundary layer and we forget about the rest of the domain. Without any surprise this strategy cannot lead to good numerical results.

α	$\beta = 1/8$		$\beta = 1/4$		$\beta = 1/2$		$\beta = 1$		$\beta = 2$	
	$\|\varepsilon_h\|_\infty$	n	$\|\varepsilon_h\|_\infty$	n	$\|\varepsilon_h\|_\infty$	n	$\|\varepsilon_h\|_\infty$	n	$\|\varepsilon_h\|_\infty$	n
0	$0.375 \cdot 10^{-2}$	1	$0.375 \cdot 10^{-2}$	1	$0.375 \cdot 10^{-2}$	1	$0.375 \cdot 10^{-2}$	1	$0.375 \cdot 10^{-2}$	1
0.1	$0.330 \cdot 10^{-2}$	6	$0.288 \cdot 10^{-2}$	7	$0.206 \cdot 10^{-2}$	8	$0.715 \cdot 10^{-3}$	12	$0.382 \cdot 10^{-2}$	35
0.5	$0.230 \cdot 10^{-2}$	8	$0.141 \cdot 10^{-2}$	10	$0.358 \cdot 10^{-3}$	13	$0.150 \cdot 10^{-2}$	22	$0.135 \cdot 10^{-1}$	92
1	$0.182 \cdot 10^{-2}$	10	$0.816 \cdot 10^{-3}$	12	$0.321 \cdot 10^{-3}$	16	$0.176 \cdot 10^{-2}$	30	$0.377 \cdot 10^{-1}$	167
2	$0.142 \cdot 10^{-2}$	10	$0.423 \cdot 10^{-3}$	15	$0.483 \cdot 10^{-3}$	22	$0.230 \cdot 10^{-2}$	42	$0.841 \cdot 10^{-1}$	699
10	$0.951 \cdot 10^{-3}$	13	$0.824 \cdot 10^{-4}$	20	$0.630 \cdot 10^{-3}$	38	$0.750 \cdot 10^{-2}$	123	0.227	73
10^2	$0.832 \cdot 10^{-3}$	14	$0.854 \cdot 10^{-5}$	22	$0.827 \cdot 10^{-3}$	46	$0.630 \cdot 10^{-1}$	45	0.204	66
10^3	$0,820 \cdot 10^{-3}$	14	$0,132 \cdot 10^{-5}$	22	$0.113 \cdot 10^{-2}$	46	$0.743 \cdot 10^{-1}$	36	0.202	65
10^4	$0.819 \cdot 10^{-3}$	14	$0.644 \cdot 10^{-6}$	23	$0.117 \cdot 10^{-2}$	46	$0.754 \cdot 10^{-1}$	37	0.202	64

Table 2. *Effect of monitoring function* (3.1) *parameters* α, β *on the accuracy of the fully converged numerical solution. Here we report also the number* n *of iterations needed to achieve the prescribed tolerance* $\varepsilon = 10^{-10}$. *Problem parameters are* $\ell = 1$, $\lambda = 10$ *and only* $N = 20$ *nodes are used.*

In order to complete the numerical study, we slightly change the monitor function to make it closer to what is actually used in practice [16]. Namely, we take the following family of monitor functions parametrized by two positive real parameters $\alpha, \beta \in \mathbb{R}_0^+$:

$$\omega_{\alpha,\beta}(x) = 1 + \alpha |u_x|^\beta, \tag{3.1}$$

where this time $u(x)$ is *not* the exact solution given in (2.2), but the solution being computed numerically. Thus, the grid generation process becomes iterative and the stopping criterium is

$$\|u_h^{n+1} - u_h^n\|_\infty < \varepsilon,$$

where ε is a tolerance parameter taken to be $\varepsilon = 10^{-10}$ in the simulations performed below. The iterative procedure is explained above in Section 2.3. A grid generated in this way will be called an *adaptive grid* to the solution with the monitor function $\omega_{\alpha,\beta}(x)$ defined in (3.1). The numerical results reported in Table 2 show that here again the lowest errors in the solution are achieved for the parameter $\beta = 1/4$. For $\beta = 1/2$ (as well as for $\beta = 1$ and $\beta = 2$) we can see that the error does not depend *monotonically* on the other parameter α. The results for $\beta = 2$ are even worse than for the corresponding uniform grid.

In general, the optimal determination of the monitoring function parameters α, β is a complex problem. In principle, one could investigate the numerical performance of even more general monitor functions such as

$$\omega(x) = 1 + \alpha_0 |u|^{\beta_0} + \alpha_1 |u_x|^{\beta_1} + \alpha_2 |u_{xx}|^{\beta_2},$$

but it is beyond the scope of the present study.

4. Explanations

In order to have some theoretical insight into the numerical results presented above (especially we would like to explain the surprising performance of the "magic" choice $\beta = 1/4$), we study the approximation properties of the scheme (2.9) on general non-uniform grids:

$$\psi_j = -\frac{1}{h_j}\left[\frac{u(x_{j+1}) - u(x_j)}{h_{j+1/2}} - \frac{u(x_j) - u(x_{j-1})}{h_{j-1/2}}\right] + \lambda^2 u(x_j).$$

The smallness of ψ_j in terms of h (the uniform step in the reference domain) will characterize the consistency error of the scheme (2.9). We assume the following

Definition 1. *The difference scheme $\mathscr{L}^h u_h = 0$ approximates the problem $\mathscr{L}u = 0$ on its solution with the order p, if there exists a constant $C = \mathrm{const}$ and a natural number $N_0 \in \mathbb{N}$ such that $\forall N \geqslant N_0$*

$$\|\psi_h\|_\infty \leqslant Ch^p.$$

Let us compute the consistency error ψ_j for the scheme (2.9). To achieve this goal we develop the solution into local Taylor expansions and composing finite differences which appear in (2.9):

$$\begin{aligned}
\frac{u(x_{j+1}) - u(x_j)}{h_{j+1/2}} &= u' + \frac{h_+}{2}u'' + \frac{h_+^2}{6}u''' + \frac{h_+^3}{24}u^{(4)} + \frac{h_+^4}{120}u^{(5)} + \mathcal{O}(h_+^5),\\
\frac{u(x_j) - u(x_{j-1})}{h_{j-1/2}} &= u' - \frac{h_-}{2}u'' + \frac{h_-^2}{6}u''' - \frac{h_-^3}{24}u^{(4)} + \frac{h_-^4}{120}u^{(5)} + \mathcal{O}(h_-^5),
\end{aligned}$$

where $h_\pm := h_{j\pm1/2}$ and the derivatives on the right hand side are evaluated at $x = x_j$. We did not specify it for the sake of compactness, but this assumption will hold below. Now we can estimate asymptotically

$$\begin{aligned}
\psi_j = -u'' + \lambda^2 u - \frac{h_+ - h_-}{3}u''' - \frac{h_+^2 - h_+h_- + h_-^2}{12}u^{(4)}\\
- \frac{(h_+ - h_-)(h_+^2 + h_-^2)}{60}u^{(5)} + \mathcal{O}(h^4), \quad (4.1)
\end{aligned}$$

where we used the fact that $\mathcal{O}(h_-^4) = \mathcal{O}(h_+^4) = \mathcal{O}(h^4)$, which follows from (2.5). Since $u(x_j)$ is the solution of (2.1), then $-u'' + \lambda^2 u \equiv 0$.

By assuming that the mapping $x(q)$ is sufficiently smooth, we obtain

$$\begin{aligned}
h_+ &= x(q_{j+1}) - x(q_j) = hx_q + \frac{h^2}{2}x_{qq} + \frac{h^3}{6}x_{qqq} + \mathcal{O}(h^4),\\
h_- &= x(q_j) - x(q_{j-1}) = hx_q - \frac{h^2}{2}x_{qq} + \frac{h^3}{6}x_{qqq} + \mathcal{O}(h^4).
\end{aligned}$$

The last two expansions allow us to estimate asymptotically the following combinations, which appear as coefficients in (4.1):

$$\begin{aligned} h_+ - h_- &= h^2\, x_{qq} + \mathcal{O}(h^4), \\ h_+^2 - h_+h_- + h_-^2 &= h^2\, x_q^2 + \mathcal{O}(h^4), \\ (h_+ - h_-)\,(h_+^2 + h_-^2) &= \mathcal{O}(h^4). \end{aligned}$$

By substituting these estimations into (4.1), one can conclude

$$\psi_j = -\frac{h^2}{3}\left[x_{qq}\, u_{xxx} + \frac{1}{4}\, x_q^2\, u_{xxxx}\right] + \mathcal{O}(h^4).$$

Thus, it shows that in general the scheme (2.9) is second order accurate. However, one can notice that the scheme will be exceptionally the fourth order accurate if the mapping $x(q)$ satisfies the following equation:

$$x_{qq}\, u_{xxx} + \frac{1}{4}\, x_q^2\, u_{xxxx} \equiv x_{qq}\, u_{xxx} + \frac{1}{4}\, x_q\, u_{xxxq} = 0, \tag{4.2}$$

where $u(x)$ is a solution to equation (2.1). Finally, we can rewrite equation (4.2) in a compact form

$$(u_{xxx})^{3/4}\left[\,(u_{xxx})^{1/4}\, x_q\right]_q = 0. \tag{4.3}$$

After noticing that $u_{xxx} \propto u_x$ thanks to (2.1), equation (4.3) can be recast into an equivalent, but more familiar form:

$$\left[\,(u_x)^{1/4}\, x_q\right]_q = 0,$$

which is to be compared with (2.10) and (2.14). This observation demystifies the surprising performance of $\beta = \frac{1}{4}$.

5. Discussion

In the present note we provided an example of a boundary value problem, which exhibits the boundary layer phenomenon, as a prototype of more complex problems arising *e.g.* in Fluid Mechanics [22]. When this equation is discretized with central finite differences on a uniform grid, one formally obtains the second order accuracy uniformly in space. However, the proportionality constant in the consistency error term becomes unacceptably large in the boundary layer. So, this solution cannot be satisfactory for more complex 3D problems. Consequently, we proposed to keep precisely the same scheme, but to modify the grid using the equidistribution principle. As a result we show first that the proportionality constant becomes quasi-uniform in space (no substantial increase in the boundary layer), but the main gain is in the order of convergence, which becomes equal to *four* provided that the mesh nodes are distributed accordingly. One can even ask a question in view of the study [7]: is it better to redistribute the nodes in order to improve substantially the scheme accuracy instead of preserving some symmetries at the discrete level? The numerical results of the present study seem to favour the former possibility.

This example is very simple and instructive since it shows how poor is our current understanding of the numerical analysis on non-uniform adaptive[1] grids. Similar techniques can be used to solve more realistic problems involving boundary layers, blow up phenomena [4] and other rapid variations in space/time of the solution. Recently we employed these techniques to solve numerically hyperbolic conservation laws [16]. From our experience it follows that one can expect a substantial improvement of the scheme properties when adaptive grids are *carefully* employed. However, the negative examples we provide show also that the application of adaptive grids does not necessarily lead *per se* to the increase in the accuracy. Consequently, the critical analysis of obtained numerical results is always needed.

The perspectives opened by this study include the description of *optimal* monitoring functions for some classes of problems. In the absence of such optimal choice, one has to describe at least the values of free parameters (*e.g.* α, β) which yield converged numerical solutions with desired properties. Here we made a proposition for a singularly perturbed Sturm–Liouville problem. However, the variety of boundary layers encountered in practice is much richer. It looks like a successful numerics can be achieved only in conjunction with deep analytical understanding of the problem in hands.

Acknowledgments

This research was supported by RSCF project No 14-17-00219. D. Dutykh acknowledges the support of the CNRS under the PEPS InPhyNiTi project FARA and project N°EDC26179 — "*Wave interaction with an obstacle*" as well as the hospitality of the Institute of Computational Technologies SB RAS during his visit in October 2015. The authors would also like to thank Prof. Laurent Gosse (CNR, Italy) for stimulating discussions on singularly perturbed Sturm–Liouville problems.

References

[1] G. B. Alalykin, S. K. Godunov, L. L. Kireyeva, and L. A. Pliner. *Solution of One-Dimensional Problems in Gas Dynamics on Moving Grids*. Nauka, Moscow, 1970. 4

[2] N. S. Bakhvalov. The optimization of methods of solving boundary value problems with a boundary layer. *USSR Computational Mathematics and Mathematical Physics*, 9(4):139–166, Jan. 1969. 4

[3] S. Barbeiro, J. A. Ferreira, and R. D. Grigorieff. Supraconvergence of a finite difference scheme for solutions in $H^s(0, L)$. *IMA J. Numer. Anal.*, 25(4):797–811, Feb. 2005. 5

[4] C. Budd and V. Dorodnitsyn. Symmetry-adapted moving mesh schemes for the nonlinear Schrödinger equation. *J. Phys. A: Math. Gen.*, 34(48):10387–10400, Dec. 2001. 4, 5, 16

[1] The grid becomes *moving* for time-dependent problems. See [16] for some examples on hyperbolic problems.

[5] C. J. Budd, B. Leimkuhler, and M. D. Piggott. Scaling invariance and adaptivity. *Appl. Numer. Math.*, 39(3-4):261–288, Dec. 2001. 5

[6] C. J. Budd and M. D. Piggott. The geometric integration of scale-invariant ordinary and partial differential equations. *J. Comp. Appl. Math.*, 128(1-2):399–422, Mar. 2001. 4

[7] M. Chhay, E. Hoarau, A. Hamdouni, and P. Sagaut. Comparison of some Lie-symmetry-based integrators. *J. Comp. Phys.*, 230(5):2174–2188, 2011. 4, 15

[8] V. A. Dorodnitsyn. Finite Difference Models Entirely Inheriting Continuous Symmetry of Original Differential Equations. *Int. J. Mod. Phys. C*, 05(04):723–734, Aug. 1994. 5

[9] R. Eymard, J. Fuhrmann, and K. Gärtner. A finite volume scheme for nonlinear parabolic equations derived from one-dimensional local dirichlet problems. *Numerische Mathematik*, 102(3):463–495, Jan. 2006. 4

[10] P. A. Farrell, J. J. H. Miller, E. O'Riordan, and G. I. Shishkin. A Uniformly Convergent Finite Difference Scheme for a Singularly Perturbed Semilinear Equation. *SIAM J. Numer. Anal.*, 33(3):1135–1149, June 1996. 4

[11] R. P. Fedorenko. *Introduction to Computational Physics*. MIPT Press, Moscow, 1994. 9

[12] J. A. Ferreira and R. D. Grigorieff. On the supraconvergence of elliptic finite difference schemes. *Appl. Numer. Math.*, 28(2-4):275–292, Oct. 1998. 5

[13] S. K. Godunov and V. S. Ryabenkii. *Difference Schemes*. North-Holland, Amsterdam, 1987. 7

[14] A. M. Il'in. Differencing scheme for a differential equation with a small parameter affecting the highest derivative. *Mathematical Notes of the Academy of Sciences of the USSR*, 6(2):596–602, Aug. 1969. 4

[15] H. B. Keller. Numerical Methods in Boundary-Layer Theory. *Ann. Rev. Fluid Mech.*, 10(1):417–433, Jan. 1978. 4

[16] G. S. Khakimzyanov, D. Dutykh, D. E. Mitsotakis, and N. Y. Shokina. Numerical solution of conservation laws on moving grids. *Submitted*, pages 1–28, 2015. 8, 13, 16

[17] P. D. Lax and R. D. Richtmyer. Survey of the stability of linear finite difference equations. *Comm. Pure Appl. Math.*, 9(2):267–293, May 1956. 7

[18] A. G. Nikitin. On the principal eigenfunction of a singularly perturbed Sturm-Liouville problem. *Zh. Vychisl. Mat. Mat. Fiz.*, 39(4):588–591, 1999. 6

[19] P. L. Roe. Computational fluid dynamics - retrospective and prospective. *International Journal of Computational Fluid Dynamics*, 19(8):581–594, Nov. 2005. 4

[20] H.-G. Roos. Ten ways to generate the Il'in and related schemes. *J. Comp. Appl. Math.*, 53(1):43–59, July 1994. 4

[21] A. A. Samarskii. *The Theory of Difference Schemes*. CRC Press, New York, 2001. 4

[22] H. Schlichting and K. Gersten. *Boundary-Layer Theory*. Springer-Verlag, Berlin, Heidelberg, 2000. 4, 5, 15

[23] G. Strang and A. Iserles. Barriers to Stability. *SIAM J. Numer. Anal.*, 20(6):1251–1257, Dec. 1983. 5

[24] V. G. Sudobicher and S. M. Shugrin. Flow along a dry channel. *Izv. Akad. Nauk SSSR*, 13(3):116–122, 1968. 4

[25] A. N. Tikhonov and A. A. Samarskii. Homogeneous difference schemes. *Zh. vych. mat.*, 1(1):5–63, 1961. 4

[26] A. N. Tikhonov and A. A. Samarskii. Homogeneous difference schemes on non-uniform nets. *Zh. vych. mat.*, 2(5):812–832, 1962. 4

[27] Y. B. Zel'dovich and Y. P. Raizer. *Physics of Shock Waves and High-Temperature Hydrodynamic Phenomena*. Dover Publications, New York, dover edition, 2002. 5

Institute of Computational Technologies, Siberian Branch of the Russian Academy of Sciences, Novosibirsk 630090, Russia
E-mail address: Khak@ict.nsc.ru
URL: http://www.ict.nsc.ru/ru/structure/Persons/ict-KhakimzyanovGS

LAMA, UMR 5127 CNRS, Université Savoie Mont Blanc, Campus Scientifique, 73376 Le Bourget-du-Lac Cedex, France
E-mail address: Denys.Dutykh@univ-savoie.fr
URL: http://www.denys-dutykh.com/